European Journal of Radiology 116 (2019) 98–105

Contents lists available at ScienceDirect

European Journal of Radiology

journal homepage: www.elsevier.com/locate/ejrad

Prognosis assessment in metastatic gastrointestinal stromal tumors treated with tyrosine kinase inhibitors based on CT-texture analysis

Kaspar Ekert[a,*], Clemens Hinterleitner[b,1], Marius Horger[a,1]

[a] Eberhard Karls University, Department of Radiology, Diagnostic and Interventional Radiology, Hoppe-Seyler-Str. 3, D-72076 Tübingen, Germany
[b] Department of Internal Medicine II, Eberhard-Karls-University, Otfried-Müller-Str. 10, 72076, Tübingen, Germany

ARTICLE INFO

Keywords:
CT textural features
GIST
TKI therapy
Therapy monitoring

ABSTRACT

Purpose: Identification of prognostic CT-textural features in patients with gastrointestinal stromal tumors undergoing tyrosine kinase inhibitor (TKI) therapy.

Methods and materials: We identified 25 GIST patients (mean age, 70.58 ± 9.7 years; range, 41.25–84.08 years; 20 males, 5 females) with a total of 123 scans, each examined with a standardized CT protocol between 1/2014 − 7/2018. 92 texture features, based on pyradiomics library, were extracted and correlated to response categories; evaluated with help of modified Choi criteria. All patients underwent therapy with imatinib in the first line and different tyrosine kinase inhibitors after disease progression. KIT and PDGFR-mutations were registered in all patients as well as the number of previous treatment regimens, patient's age as well as gender and the presence of contrast enhancement (vitality) in tumor. The lesion with the largest diameter was chosen and contoured using the spherical VOI tool. Inter-rater testing was performed by a second experienced radiologist. Regression and AUC analysis was performed.

Results: Ten variables could be confirmed to be significantly associated with disease progression. Of them, four textural parameters were significantly positively associated with disease progression and negatively with progression free survival (Glcm Id [grey-level co-occurrence matrix inverse difference], p = 0.012, HR 3.83; 95% CI 1.697–8.611, Glcm Idn [grey-level co-occurrence matrix inverse difference normalized], p = 0.045, HR 2.06, 95% CI 1.015–4.185, Glrlm [grey-level run length matrix] normalized, p = 0.005, HR 3.181; 95% CI 1.418–7.138 and Ngtdm [neighboring grey-tone difference matrix] coarseness, p < 0.001, HR 3.156, 95% CI 1.554–6.411). Single variables were shown to be significantly inferior to the combination of all variables. After 6 months, 90% of patients with 0–1 risk factors (group 1), 64.4% with 2–3 risk variables and 38.1% of patients presenting > 3 structural risk variables showed stable disease. Gclm Id, Gclm Idn and Glrlm non-uniformity were associated with the number of previous treatments, Glrlm non-uniformity also with tumor vitality (enhancement), whereas Gclm Idn and Ngtdm coarseness were associated with the number of tumor mutations.

Conclusion: Some of the CT-textural features correlate with disease progression and the progressive free survival as well as with the number of gene mutations and the number of treatment regimens the patients were exposed to as well as with the tumor enhancement. All these features reflect tumor homogeneity.

1. Introduction

Gastrointestinal stromal tumors (GIST) are rare mesenchymal non-epithelial tumors arising from the Cajal interstitial cells of the GI-tract [1]. Mutations of the c-KIT are the crucial step for the development of a GIST, but other mutated genes have also been identified (e.g. PDGFR-α) [2]. Based on this knowledge, targeted drugs against these receptors have been developed and by now successfully implemented in the therapeutic armamentarium for GIST [3,4]. Many of the tyrosine kinase inhibitors (TKI) knowingly have also antiangiogenic effects blocking the vascular endothelial growth factor receptors (VEGFR) leading in most responders to a drop in blood supply and consequently to necrosis and cystic transformations of these tumors that are otherwise well vascularized [5]. Based on this knowledge, specific response criteria have been proposed which consider not only size changes induced by therapy but also such reflecting tumor perfusion and attenuation [5].

* Corresponding author.
E-mail addresses: kaspar.ekert@med.uni-tuebingen.de (K. Ekert), clemens.hinterleitner@med.uni-tuebingen.de (C. Hinterleitner), marius.horger@med.uni-tuebingen.de (M. Horger).
[1] Both authors share equal contribution.

https://doi.org/10.1016/j.ejrad.2019.04.018
Received 4 February 2019; Received in revised form 22 March 2019; Accepted 27 April 2019

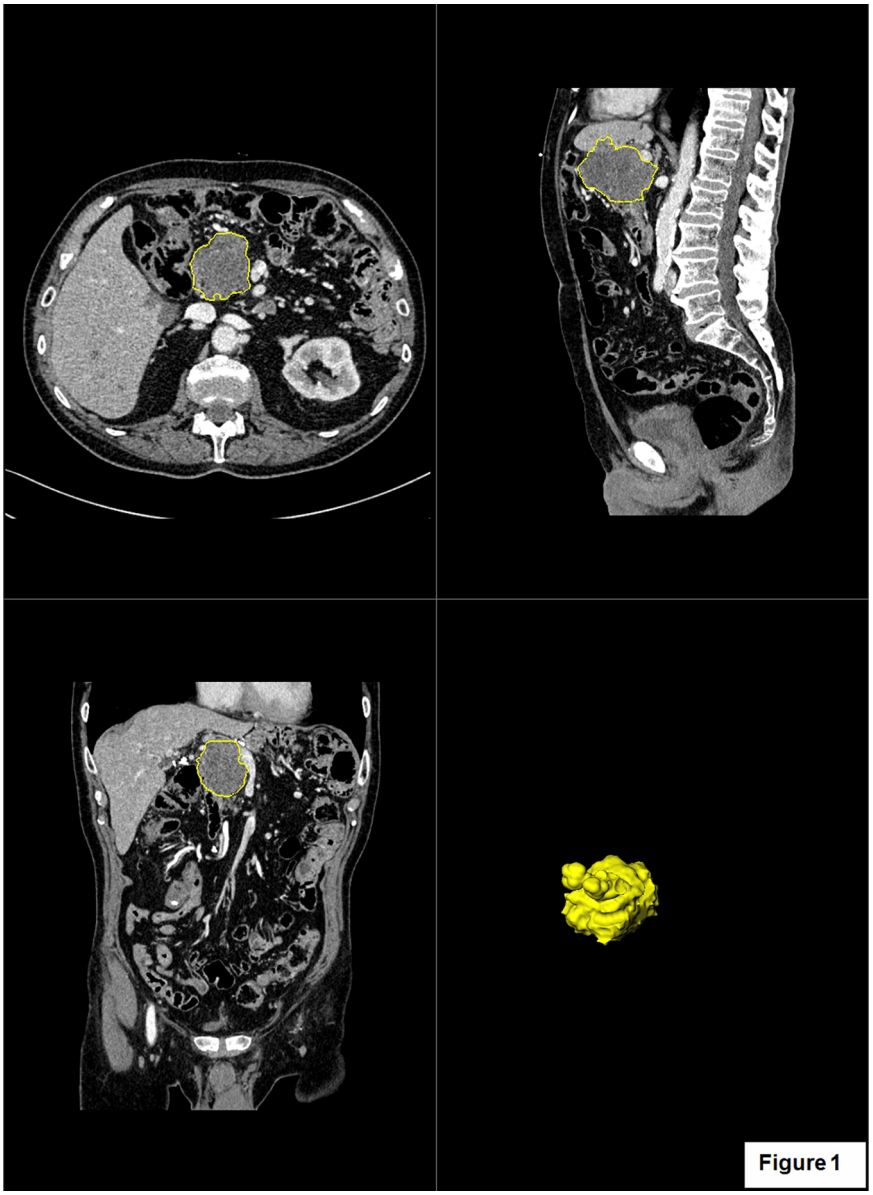

Fig. 1. Multiplanar image annotation and 3D reformat of the segmented GIST lesion. From the resulting volume of interest CT textural features are extracted.

CT is the mainstay in the diagnostic and response monitoring of GIST to TKI, but other less frequently involved imaging modalities (e.g. MRI, FDG-PET) have also been successfully tested in this clinical setting [6–8]. The main role of imaging is to possibly assess all GIST-manifestations for treatment planning (e.g. surgery vs. systemic treatment) as well as to monitor therapy, predict malignancy risk and prognosis [9,10]. The latter has been already tested using early FDG-PET monitoring, however without success [11].

CT-texture analysis (CTTA) is one part of the radiomics spectrum which delivers quantitative data on tumor heterogeneity by analyzing the distribution and relationship of voxel grey levels in the image [12]. It is based on histogram analysis and comprises different order statistic features that finally all reflect tissue heterogeneity. Contrast enhanced CT (CECT)-data is employed for the diagnostic work-up of GIST and therefore CTTA-results are additionally influenced by the vascular network [13]. For evaluation of well perfused cancerous lesions like the GISTs, focusing on textural changes additionally to visual assessment of drug-related vascular changes (according to CHOI criteria) in the tumor seems plausible.

The aim of this study was to determine the prognostic value of CT-textural features by comparing them with the progressive free survival in our cohort. Moreover, potential associations between textural features, the number of past treatment regimens as well as the tumor mutation status and the tumor vitality (presence of enhancement) were also evaluated.

2. Materials and methods

2.1. Subjects

The ethics committee at our institution approved this study. We identified a total of 153 GIST patients at our institution; however, most patients had to be excluded since many provided inadequate (non-standardized) image data (mostly missing thin collimation data). In the end, 25 GIST patients (mean age, 70.58 ± 9.7 years; range, 41.25–84.08 years; 20 males, 5 females) with 123 CT-examinations fulfilled enrollment criteria. Each patient was examined using a standardized CT protocol between 1/2014 − 7/2018. All patients had histological work-up including the KIT and PDGFR mutation status. 92 texture features, based on pyradiomics library [25], were extracted and correlated to response category evaluated using modified Choi criteria

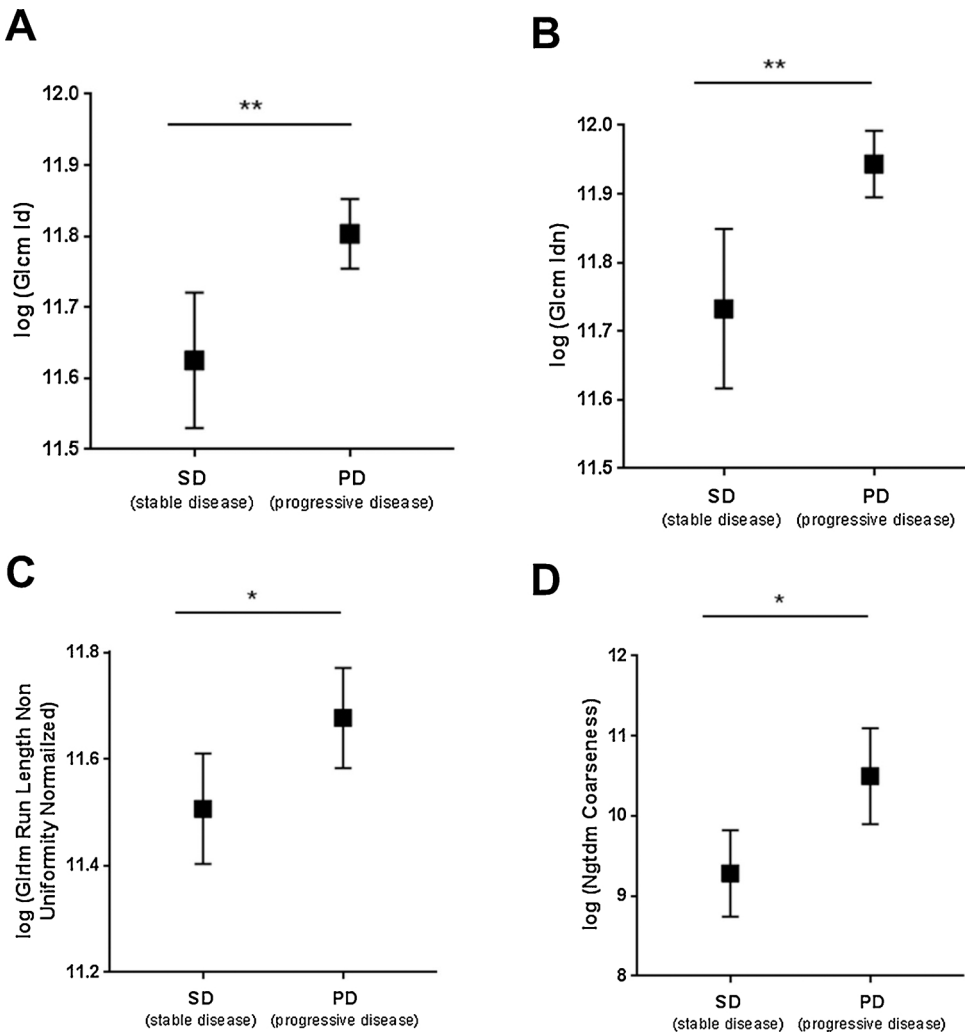

Fig. 2. Four significant structural features, highest correlation coefficients ($\eta > 0.2$) of all assessed features, presented with their logarithmic values for stable and progressive disease. Glcm Id: stable disease [SD] 11.62 vs. progressive disease [PD] 11.8, p = 0.008, Glcm Idn: SD 11.73 vs. PD 11.94, p = 0.007, Glrlm non-uniformity normalized: stable disease (SD) 11.5 vs. PD 11.68, p = 0.028, Ngtdm coarseness: SD 9.28 vs. PD 10.49, p = 0.005. For explanation of features refer to suppl. Table 1.

[26]. Patients underwent therapy with up to seven different tyrosine kinase inhibitors during their treatment (all patients receiving first line therapy with imatinib). At the time of monitoring most scans were acquired (49/123) during the 1st line of therapy; as many scans were obtained (50/123) in the 2nd and 3rd line of therapy.

2.2. CT examinational protocol

All patients were examined using either a 128 or 256-slice MDCT scanner (SOMATOM Definition AS + or SOMATOM Definition Flash, Siemens Healthcare, Forchheim, Germany) using 128 × 0.6 mm collimation, 0.5 s rotation time, 120 kV tube voltage and 200–250 mA s effective tube current time product. Contrast enhanced CT was acquire in the early portal venous phase (65 s post contrast application) using 100 ml Ultravist 370 (Bayer Vital Leverkusen, Germany) and an injection rate of 2 ml/s. A soft spatial resolution kernel (B31f) was chosen to reconstruct the data with 1 mm slice thickness in a 512 × 512 image matrix.

2.3. Overall tumor response using modified CHOI criteria

The overall tumor response on CT was determined subjectively by a consensus opinion of two radiologists (H.M. and E.K.) with 25 and 3 years of experience in abdominal imaging on the basis of the size and number of tumors, the degree and extent of enhancement, the presence or absence of tumor vessels, and the presence or absence of solid nodules within the tumors in each patient guided by the modified CHOI-criteria [26].

The lesion with the largest diameter was chosen and contoured using the spherical VOI tool of the employed radiomics prototype. Special attention was paid not to include adjacent soft tissue, e.g. gastric wall with similar density properties. All tumor parts were included in the VOI, i.e. contrast attenuated areas as well as cystic non-contrast enhanced lesions (refer to Fig. 1). Mean volume of interest (VOI) was 68.12 ml (min: 1.34 ml, max: 982.41 ml).

In addition, tumour lesions' vitality was classified in a binary fashion in regard to the presence of contrast enhancement. The representative lesion was classified non-vital only if there was no enhancement in any of the patient's lesions.

2.4. CT-textural features

92 primary features were extracted (see suppl. Table 1 for a full list of features and their definitions). Filtered features were excluded considering the small patient size. In addition, shaped based features were excluded to concentrate on the textural analysis and to further reduce the number of features.

2.5. Clinical variables potentially associated with prognosis

In a first step each variable was assigned a point score (1 = > calculated cut-off levels, 0 = < calculated cut-off level). In a second step the accuracy of all variables and the composite variable score was analyzed using receiver-operator-characteristic curve (ROC) analysis.

2.6. Statistical analysis

Continuous variables are presented as median and 95% CI, categorical variables are given by number and percentages. In all cases (n = 123) binary logistic regression analysis was used to identify variables significantly associated with disease progression and vitality. Prior regression analysis log transformation was performed in all structural parameters. The effect size was analyzed using Spearman correlation coefficient (r). For all variables without well-established cut-off levels, Youden's J statistic was used here. Finally, the predictive values of all identified parameters were evaluated by examining the area under the receiver-operator characteristic (ROC) curve, using a confidence interval of 95%. All tests were considered statistically significant when P < .05. Statistical analyses were computed using SigmaStat, version 21 (SPSS).

3. Results

3.1. Identification of CTTA-features associated with disease progression

In order to identify relevant textural features associated with disease progression, binary logistic regression analysis was used for all CT-textural features (n = 92).

In a first step ten features could be confirmed to be significantly associated with disease progression (Suppl. Table 2). Interestingly, Glcm (grey-level co-occurrence matrix), Gldm (grey-level dependence matrix) and Glrlm (grey-level run *length matrix)* group variables represented the most consistent subtypes (80%). Out of these, four structural variables reaching a correlation coefficient (η > 0.2) were further analyzed. As shown in Fig. 2, patients experiencing disease progression showed significant higher values in all four variables (Glcm Id: stable disease [SD] 11.62 vs. progressive disease [PD] 11.8, p = 0.008, Glcm Idn: SD 11.73 vs. PD 11.94, p = 0.007, Glrlm non-uniformity normalized: stable disease (SD) 11.5 vs. PD 11.68, p = 0.028, Ngtdm coarseness: SD 9.28 vs. PD 10.49, p = 0.005).

3.2. CTTA-features as predictive markers in GIST

The predictive role of the statistically significant textural features was further evaluated by the Kaplan-Meier method. The median follow-up for monitoring progression free survival (PFS) was 6 months (range: 1–49 months). Due to the lack of well-established cut-off levels Youden's J statistic was performed for all variables and amounted to 11.84 for Glcm Id, 11.98 for Glcm Idn, 11.64 for Glrlm non- uniformity normalized and 11.51 for Ngtdm coarseness.

As presented in Fig. 3, all four structural parameters were significantly associated with disease progression (positively) and progression free survival (negatively) (Glcm Id, p = 0.012, HR 3.83; 95% CI 1.697–8.611, Glcm Idn, p = 0.045, HR 2.06, 95% CI 1.015–4.185, Glrlm non-uniformity normalized, p = 0.005, HR 3.181; 95% CI 1.418–7.138 and Ngtdm coarseness, p < 0.001, HR 3.156, 95% CI 1.554–6.411).

3.3. Combined textural analysis increases predictive power for disease progression

Considering the data of the individual follow-up analysis (Fig. 4a–b), a combination of several variables seems to be a promising approach for an optimized prediction of disease progression. Remarkably, the single variables were shown to be significantly inferior to the combination of all variables (Glcm Id, p = 0.006, AUC 0.649; 95% CI 0.545 − 0.754, Glcm Idn, p = 0.001, AUC 0.686; 95% CI 0.586 − 0,786, Glrlm Run Length non-uniformity normalized,

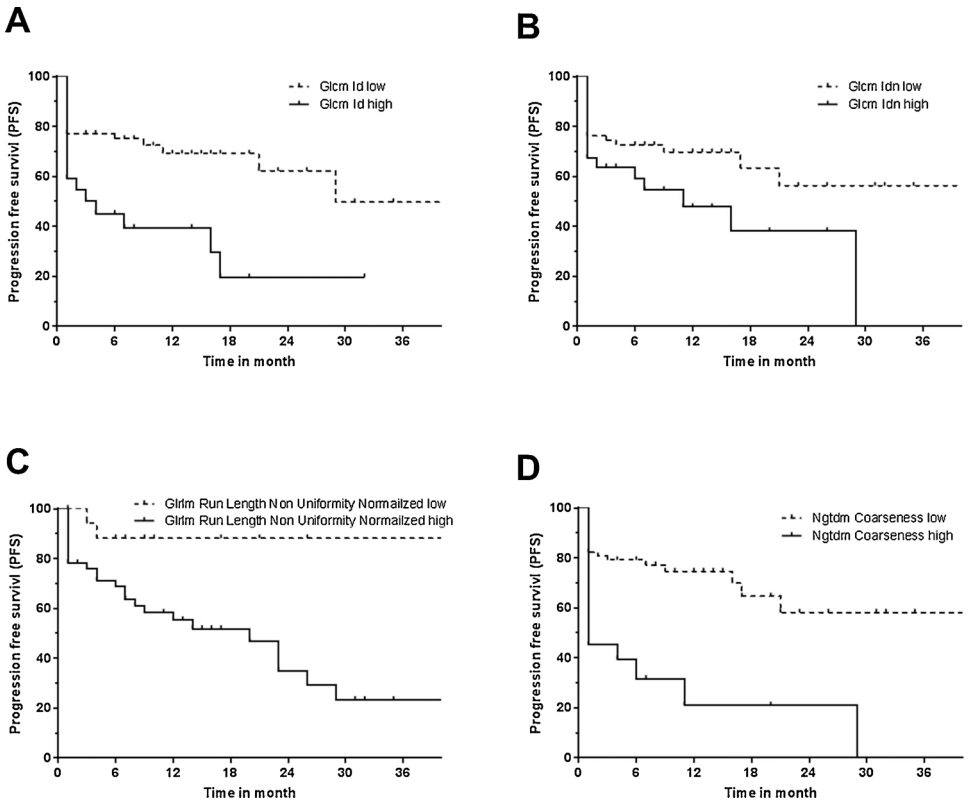

Fig. 3. Predictive role of the four significant structural features using Kaplan-Meier diagrams. Low and high significance refers to the calculated cut-off levels for each feature using Youden's J statistic. Calculated cut-off levels amounted to 11.84 for Glcm Id, 11.98 for Glcm Idn, 11.64 for Glrlm non- uniformity normalized and 11.51 for Ngtdm coarseness. Features were positively associated with disease progression and negatively with progression free survival. For explanation of features refer to suppl. Table 1.

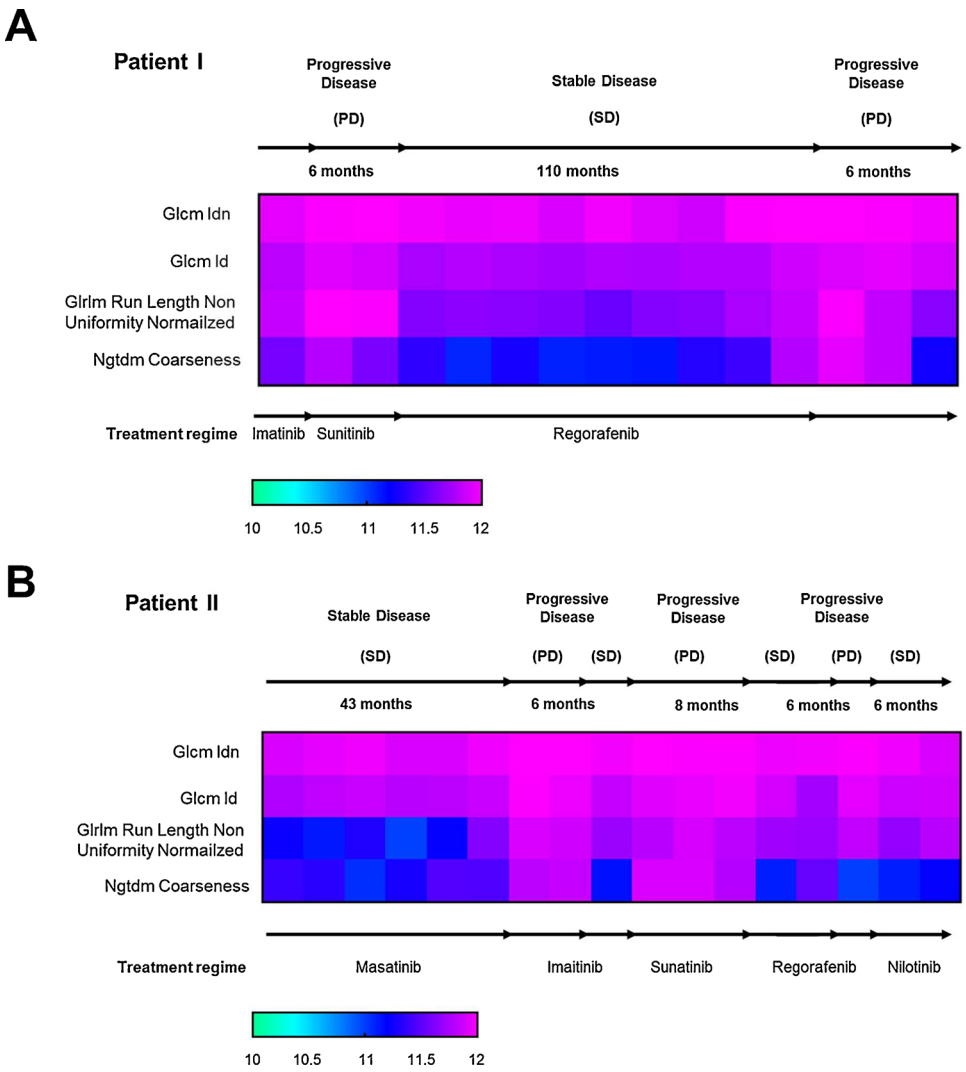

Fig. 4. Exemplary therapy monitoring in two patients receiving different tyrosine kinase inhibitors using the four significant textural features. Blue colors representing lower values for the four significant features and pink colors higher values (i.e. disease progression positively correlated with the four features). For explanation of features refer to suppl. Table 1.

$p = 0.002$, AUC 0.626; 95% CI 0.526 − 0.726, Ngtdm coarseness, $p < 0.001$, AUC 0.7; 95% CI 0.6 − 0.8 vs. combined variables, < 0.001, AUC 0.827, 95% CI 0.755 − 0.9). Finally three risk-factor groups (group 1: 0–1 positive variables [features], group 2: 2–3 positive variables and group 3: > 3 positive variables) were defined and correlated with the progression free survival (PFS). As shown in Fig. 5b, after 6 months 90% of patients with 0–1 risk factor (group 1) showed a stable disease. In contrast only 64.4% of patients with 2 or 3 positive risk variables and 38.1% of patients presenting more than 3 structural risk variables showed a stable disease after 6 months of treatment. Moreover, the median PFS was not reached in group 1 whereas group 2 showed 17 months and group 3 only two months ($p < 0.0001$).

3.4. Association of textural parameters with clinical parameters in GIST

Grey-level co-occurrence matrix inverse difference levels proved to be significantly ($p < 0.001$) associated with the number of previous treatment regimens and in particular with the agent nilotinib (refer to Table 1). There was no other significant correlation with patient's age, gender, presence of tumor enhancement (vitality) or the number of GIST mutations.

Grey-level co-occurrence matrix inverse difference normalized levels were significantly associated with the number of past treatment regimens and in particular with the agent nilotinib, but interestingly also with the number of GIST mutations (refer to Table 2). Patient's age, gender and the presence of tumor enhancement (vitality) did not yield significant correlations.

Grey-level run length matrix non-uniformity normalized levels revealed significant associations with the number of past treatment regimens and in particular with the agent sunitinib as well as with the presence of tumor enhancement (vitality) (refer to Table 3). There was no significant correlation with the patient's age, gender or the number of mutations.

Neighboring grey-tone difference matrix coarseness levels were significantly associated with the number of GIST mutations (refer to Table 4).

3.5. Structural variables in individual follow-up analysis

Fig. 4a and b represent individual temporal courses of the four textural features in two GIST patients undergoing subsequent different TKI-therapies.

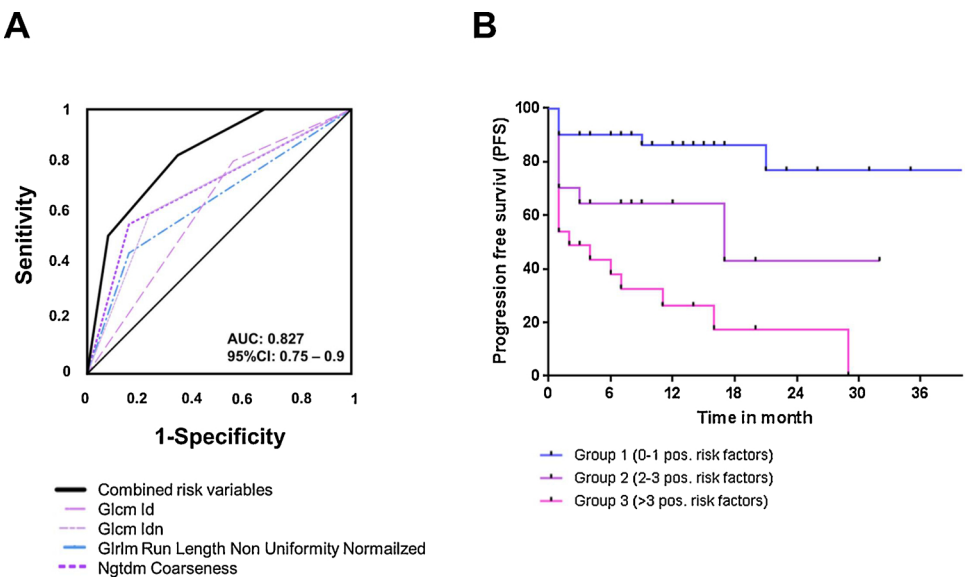

Fig. 5. Combination of features. A) ROC analysis for all four features and their combined score of 0.827 (95% CI: 0.75 – 0.9). B) Three risk-factor groups (group 1: 0–1 positive variables [features], group 2: 2–3 positive variables and group 3: > 3 positive variables) correlating them with progression free survival (PFS) in Kaplan-Meier diagram. For explanation of features refer to suppl. Table 1.

Table 1
Association of Glcm Id (grey-level co-occurrence matrix inverse difference) with clinical parameters.

Patient characteristics	Glcm Id		
	negative (n = 94)	positive (n = 27)	*p value*
Gender			
male sex, %	43	57	*0.41*
Age			
years, mean – yr.(SD)	67.3 ± 9.2	64.3 ± 10.5	*0.42*
Vital tumor lesion – n (%)	55 (58%)	16 (59%)	*0.94*
Number of mutations			
n – (95% CI)	1 (1.26–1.72)	1 (1–1.52)	*0.31*
Number of treatment regimens exposed to			
median – (95% CI)	2 (1.62–2.14)	3 (2.22–3.64)	*0.001*
Treatment			
Imatinib	33 (35.1)	13 (48.1)	
Masitinib	6 (6.4)	2 (7.4)	
Nilotinib	4 (4.3)	2 (7.4)	*0.66*
Sunitinib	19 (20.2)	5 (18.5)	
Regorafenib	24 (25.5)	5 (18.5)	
Sorafenib	2 (2.1)	0	

Table 2
Association of Glcm Idn (grey-level co-occurrence matrix inverse difference normalized) with clinical parameters.

Patient characteristics	Glcm Idn		
	negative (n = 78)	positive (n = 43)	*p value*
Gender			
male sex, %	55	45	*0.32*
Age			
years, mean– yr.(SD)	64.1 ± 10.4	66.7 ± 9.4	*0.34*
Vital tumor lesion – n (%)	43 (55%)	28 (64%)	*0.29*
Number of mutations			
n – (95% CI)	1 (1–1.39)	2 (1.53–2.24)	*< 0.001*
Number of treatment regimens exposed to			
median – (95% CI)	1 (1.52–2.01)	3 (2.2–3.2)	*0.001*
Treatment, n (%)			
Imatinib	31 (39.7)	15 (34.9)	
Masitinib	8 (10.3)	0	
Nilotinib	1 (1.3)	5 (11.6)	*0.03*
Sunitinib	17 (21.8)	7 (16.3)	
Regorafenib	16 (20.5)	13 (30.2)	
Sorafenib	2 (2.6)	0	

4. Discussion

This study employed CT texture analysis acquired in the portal-venous phase for prediction of response of gastrointestinal stromal tumors to tyrosine kinase inhibitors as well as for their characterization in terms of tissue vitality (presence of enhancement). Further potential associations were drawn with tumor gene mutations, the number of pre-treatments and patient's age as well as gender.

In our series all patients with progressive disease showed significant higher levels of second order (grey-level co-occurrence matrix inverse difference and inverse difference normalized) and higher order (neighboring grey-tone coarseness and grey-level run length matrix) textural features. All these parameters describe one central image (i.e. tissue) characteristic in the form of homogeneity. Nowadays calculated abstract features allow conclusions about homogeneity in an objective manner, previously assessed in a subjective visual manner. For that matter, Glcm (grey-level co-occurrence matrix inverse difference) represents a measure of the local homogeneity of an image with Glcm inverse difference (ID) focusing on the difference between the neighboring intensity values dividing over the total number of discrete intensity values; likewise Glcm ID normalized (grey-level co-occurrence matrix inverse difference normalized) corrected for outliers. The Ngtdm coarseness (neighboring grey-tone difference matrix coarseness) measures the average differences between the center voxel and its adjacent neighbors being an indicator of the spatial rate of change; higher values indicating a more uniform texture. Lastly, Glrlm non-uniformity normalized (Gray level run-length non-uniformity normalized) measures the similarity of run lengths throughout the image, corrected for outliers. The other textural features that were significantly associated with disease progression (Gclm contrast, Gclm sum average, grey-level dependence matrix (Gldm) variance and large dependence emphasis) and grey-level size zone matrix (Glszm) non-uniformity in our series are also measures of the voxel intensity (tissue) composition, however singular and with no overreaching deducible pattern.

Nonetheless, our results are surprising as in most reports about image (tissue) texture analysis the opposite of tissue homogeneity, the spatial heterogeneity in cellular density, vascularization and necrosis was found to correlate with biologically aggressive malignant tumors and such that are often resistant to therapy [11]. Ganeshan et al. described higher degrees of tumor heterogeneity in clinical stage III and

Table 3
Association of Glrlm Run Length Non Uniformity Normalized with clinical parameters.

Patient characteristics	Glrlm Run Length Non Uniformity Normalized		
	negative (n = 28)	positive (n = 93)	*p value*
Gender			
male sex, %	38	62	*0.36*
Age			
years, mean– yr.(SD)	66.4 ± 9.3	63,.9 ± 9.1	*0.68*
Vitality in %			
mean – (95% CI)	3 (10.7)	68 (73.1)	*< 0.001*
Number of mutations			
n – (95% CI)	1 (1–1.71)	1 (1.24–1.68)	*0.64*
Number of treatment regimens exposed to			
median – (95% CI)	1 (0.86–1.35)	2 (2.11–2.73)	*< 0.001*
Treatment, n (%)			
Imatinib	16 (57.1)	30 (32.3)	
Masitinib	4 (14.3)	4 (4.3)	
Nilotinib	0	6 (6.5)	
Sunitinib	5 (17.9)	19 (20.4)	*0.02*
Regorafenib	0	29 (31.2)	
Sorafenib	0	2 (2.2)	

Table 4
Association of Ngtdm (neighboring grey-tone difference matrix) coarseness with clinical parameters.

Patient characteristics	Ngtdm Coarseness		
	negative (n = 90)	positive (n = 31)	*p value*
Gender			
male sex, %	69	53	*0.22*
Age			
years, mean– yr.(SD)	66.1 ± 8.7	64.2 ± 10.1	*0.42*
Vital tumor lesion – n (%)	49 (54%)	22 (71%)	*0.107*
Number of mutations			
median – (95% CI)	1 (1–1.42)	2 (1.6–2.46)	*< 0.001*
Number of treatment regimens exposed to			
median – (95% CI)	1 (1.68–2.3)	3 (1.97–3)	*0.104*
Treatment n – (%)			
Imatinib	36 (40)	10 (32.3)	
Masitinib	8 (8.9)	0	
Nilotinib	5 (5.6)	1 (3.2)	*0.37*
Sunitinib	18 (20)	6 (19.4)	
Regorafenib	18 (20)	11 (35.5)	
Sorafenib	1 (1.1)	1 (3.2)	

IV of esophageal carcinomas [12]. The same authors found that a coarse texture was the best discriminator between high and low grade gliomas [13]. Among the most frequent renal tumors, the most aggressive clear-cell carcinomas proved to be also the most heterogeneous [14].

With respect to GIST, CTTA has already been successfully used for evaluation of malignancy risk by Liu et al. [15]. These authors found in particular that the tumor entropy significantly correlates with the risk of malignant transformation. The same researcher's group found significant correlation between the expression of E-cadherin and standard deviation, width, entropy, derived from the arterial and venous contrast phases in gastric cancers [16]. Nevertheless, Feng et al. found that GIST-entropy as a measure of irregularity of grey-level distribution was higher in low-risk GIST compared to low-risk GIST [17]. These results could be confirmed for both arterial and portal-venous CT-phases and presumably explain in part our own results. Ng et al. described similar findings in colorectal cancer where higher tumor uniformity heralded poorer prognosis [18].

During targeted therapy of GIST, structural changes consistent with hemorrhage, necrosis, myxoid degeneration, and calcification are expected in responders whereas in non-responders or relapsing tumors increased cellularity with consecutive increase in tumor homogeneity has been observed [19]. Previous reports have stressed the role of imaging for evaluation of GIST-response to targeted agents pointing in particular to the known limitations of size-based measurements and advocating the use of combined morphologic-functional imaging like FDG-PET-CT or MRI including diffusion-weighted imaging [20,9]. A potential alternative to multimodality diagnosis could be represented by CT-textural analysis in conjunction with morphologic image evaluation using the current response recommendation based on CHOI's criteria [20]. Current experience with CTTA shows that some of the textural features have advanced to quantitative imaging biomarkers. However, variability of different tumor types in with respect to textural features as well as differences in the way these tumors respond to modern therapeutic agents are vast and for this reason, awareness of variability of imaging fingerprints is mandatory for using them properly in the clinical routine [11]. Whereas changes in GIST attenuation during successful therapy are known to have prognostic value, prediction of response based on textural features has not yet been analyzed. Using Kaplan-Meier tests our data demonstrates strong association between four of the textural features and the progression-free survival. Moreover, we found that with increasing number of risk features, the progression-free survival becomes significantly shorter. Similar attempts have been reported in patients with other tumors using CT texture analysis for response prediction [21,22]. Hence, Eilaghi et al. found that dissimilarity and inverse difference normalized represent good prognostic imaging biomarkers in patients with pancreatic ductal adenocarcinoma [23]. Ganeshan et al. reported about the supporting role of CT textural analysis for response prediction in patients with Hodgkin's lymphoma undergoing CTTA and FDG-PET ad interim, showing that textural features provide prognostic information complementary to FDG-PET [24].

Our results show that tissue homogeneity in metastatic GISTs negatively correlates with progression-free survival during TKI-treatment and significantly correlates with tumor progression. This knowledge could be implemented in the routine analysis of image data of GIST patients for outcome prediction. Whether the textural features assessed in our series represent true cellular homogeneity of the tumor lesions or their vascular network cannot be elucidated.

Furthermore, some of the textural features (Ngtdm coarseness, Gclm Idn and Glrlm non-uniformity) seem to non-invasively predict the mutation status of these tumors. We additionally found that Gclm Id, Gclm Idn and Glrlm non-uniformity were strongly associated with the number of previous treatment regimens, whereas Glrlm non-uniformity was significantly associated with the presence of tumor enhancement (vitality). Consequently, the use of CTTA-features complementary to the established morphologic imaging parameters is expected to improve prognosis in GIST patients and also enables development and implementation of e.g. computer-aided programs using post-processing-tools for PFS-evaluation. Finally, a more individualized tumor response monitoring by means of CTTA as presented in our complementary Fig. 4 could make treatment surveillance more manageable.

Our study has some limitations. First, the number of analyzed patients was low impacting statistical analysis and thus larger cohorts should be examined to confirm the trend found in this preliminary study. Second, the clinical settings differed depending on the therapy line. Third, there was no macroscopic histology correlation during treatment for understanding the true causes for increased tumor homogeneity.

In conclusion, some CT-textural features correlate with disease progression and the progressive free survival as well as with the number of gene mutations and the number of treatment regimens the patients were exposed to and the tumor enhancement. All of them reflect tumor homogeneity.

Conflicts of interest

Kaspar Ekert and Clemens Hinterleitner have no conflicts of interest.

Marius Horger received institutional research support from Siemens Healthineers Germany. He is a scientific advisor of Siemens and has received speaker's honorarium from Siemens Healthineers Germany.

Appendix A. Supplementary data

Supplementary material related to this article can be found, in the online version, at doi:https://doi.org/10.1016/j.ejrad.2019.04.018.

References

[1] M. Miettinen, J. Lasota, Gastrointestinal stromal tumors: pathology and prognosis at different sites, Semin. Diagn. Pathol. 23 (May (2)) (2006) 70–83 Review.

[2] P.J. Oppelt, A.C. Hirbe, B.A. Van Tine, Gastrointestinal stromal tumors (GISTs): point mutations matter in management, a review, J. Gastrointest. Oncol. 8 (June (3)) (2017) 466–473.

[3] V. Kasireddy, M. von Mehren, Emerging drugs for the treatment of gastrointestinal stromal tumour, Expert Opin. Emerg. Drugs 22 (December (4)) (2017) 317–329.

[4] J. Vadakara, M. von Mehren, Gastrointestinal stromal tumors: management of metastatic disease and emerging therapies, Hematol. Oncol. Clin. North Am. 27 (October (5)) (2013) 905–920.

[5] H. Choi, Imaging modalities of gastrointestinal stromal tumors, J. Surg. Oncol. 104 (December (8)) (2011) 907–914.

[6] L. Tang, J. Li, Z.Y. Li, X.T. Li, J.F. Gong, J.F. Ji, Y.S. Sun, L. Shen, MRI in predicting the response of gastrointestinal stromal tumor to targeted therapy: a patient-based multi-parameter study, BMC Cancer 18 (August (1)) (2018) 811.

[7] A. Dimitrakopoulou-Strauss, U. Ronellenfitsch, C. Cheng, L. Pan, C. Sachpekidis, P. Hohenberger, T. Henzler, Imaging therapy response of gastrointestinal stromal tumors (GIST) with FDG PET, CT and MRI: a systematic review, Clin. Transl. Imaging 5 (3) (2017) 183–197.

[8] H. Choi, Role of imaging in response assessment and individualised treatment for sarcomas, Clin. Oncol. (R. Coll. Radiol.) 29 (August (8)) (2017) 481–488.

[9] L. Tang, J. Li, Z.Y. Li, X.T. Li, J.F. Gong, J.F. Ji, Y.S. Sun, L. Shen, MRI in predicting the response of gastrointestinal stromal tumor to targeted therapy: a patient-based multi-parameter study, BMC Cancer 18 (August (1)) (2018) 811.

[10] M. Chacón, M. Eleta, A.R. Espindola, E. Roca, G. Méndez, S. Rojo, C. Pupareli, Assessment of early response to imatinib 800 mg after 400 mg progression by ^{18}F-fluorodeoxyglucose PET in patients with metastatic gastrointestinal stromal tumors, Future Oncol. 11 (6) (2015) 953–964.

[11] M.G. Lubner, A.D. Smith, K. Sandrasegaran, D.V. Sahani, P.J. Pickhardt, CT texture analysis: definitions, applications, biologic correlates, and challenges, Radiographics 37 (September-October (5)) (2017) 1483–1503.

[12] B. Ganeshan, K. Skogen, I. Pressney, D. Coutroubis, K. Miles, Tumour heterogeneity in oesophageal cancer assessed by CT texture analysis: preliminary evidence of an association with tumour metabolism, stage, and survival, Clin. Radiol. 67 (February (2)) (2012) 157–164.

[13] K. Skogen, B. Ganeshan, C. Good, G. Critchley, K. Miles, Measurements of heterogeneity in gliomas on computed tomography relationship to tumour grade, J. Neurooncol. 111 (January (2)) (2013) 213–219.

[14] L. Yan, Z. Liu, G. Wang, Y. Huang, Y. Liu, Y. Yu, C. Liang, Angiomyolipoma with minimal fat: differentiation from clear cell renal cell carcinoma and papillary renal cell carcinoma by texture analysis on CT images, Acad. Radiol. 22 (September (9)) (2015) 1115–1121.

[15] S. Liu, X. Pan, R. Liu, H. Zheng, L. Chen, W. Guan, H. Wang, Y. Sun, L. Tang, Y. Guan, Y. Ge, J. He, Z. Zhou, Texture analysis of CT images in predicting malignancy risk of gastrointestinal stromal tumours, Clin. Radiol. 73 (March (3)) (2018) 266–274.

[16] S. Liu, H. Shi, C. Ji, W. Guan, L. Chen, Y. Sun, L. Tang, Y. Guan, W. Li, Y. Ge, J. He, S. Liu, Z. Zhou, CT textural analysis of gastric cancer: correlations with immunohistochemical biomarkers, Sci. Rep. 8 (August (1)) (2018) 11844.

[17] C. Feng, F. Lu, Y. Shen, A. Li, H. Yu, H. Tang, Z. Li, D. Hu, Tumor heterogeneity in gastrointestinal stromal tumors of the small bowel: volumetric CT texture analysis as a potential biomarker for risk stratification, Cancer Imaging 18 (December (1)) (2018) 46.

[18] F. Ng, B. Ganeshan, R. Kozarski, K.A. Miles, V. Goh, Assessment of primary colorectal cancer heterogeneity by using whole-tumor texture analysis: contrast-enhanced CT texture as a biomarker of 5-year survival, Radiology 266 (January (1)) (2013) 177–184.

[19] X. Hong, H. Choi, E.M. Loyer, R.S. Benjamin, J.C. Trent, C. Charnsangavej, Gastrointestinal stromal tumor: role of CT in diagnosis and in response evaluation and surveillance after treatment with imatinib, Radiographics 26 (March-April (2)) (2006) 481–495.

[20] H. Choi, Response evaluation of gastrointestinal stromal tumors, Oncologist 13 (Suppl 2) (2008) 4–7.

[21] F. Davnall, C.S. Yip, G. Ljungqvist, M. Selmi, F. Ng, B. Sanghera, B. Ganeshan, K.A. Miles, G.J. Cook, V. Goh, Assessment of tumor heterogeneity: an emerging imaging tool for clinical practice? Insights Imaging 3 (December (6)) (2012) 573–589.

[22] C. Kloth, W.M. Thaiss, R. Kärgel, R. Grimmer, J. Fritz, S.D. Ioanoviciu, D. Ketelsen, K. Nikolaou, M. Horger, Evaluation of texture analysis parameter for response prediction in patients with hepatocellular carcinoma undergoing drug-eluting bead transarterial chemoembolization (DEB-TACE) using biphasic contrast-enhanced CT image data: correlation with liver perfusion CT, Acad. Radiol. 24 (November (11)) (2017) 1352–1363.

[23] A. Eilaghi, S. Baig, Y. Zhang, J. Zhang, P. Karanicolas, S. Gallinger, F. Khalvati, Haider MACT texture features are associated with overall survival in pancreatic ductal adenocarcinoma—a quantitative analysis, BMC Med. Imaging 17 (June (1)) (2017) 38.

[24] B. Ganeshan, K.A. Miles, S. Babikir, R. Shortman, A. Afaq, K.M. Ardeshna, A.M. Groves, I. Kayani, CT-based texture analysis potentially provides prognostic information complementary to interim fdg-pet for patients with hodgkin's and aggressive non-hodgkin's lymphomas, Eur. Radiol. 27 (March (3)) (2017) 1012–1020.

[25] J.M. van Griethuysen Joost, et al., Computational radiomics system to decode the radiographic phenotype, Cancer Res. 77 (November (21)) (2017) e104–7.

[26] Haesun Choi, et al., Correlation of computed tomography and positron emission tomography in patients with metastatic gastrointestinal stromal tumor treated at a single institution with imatinib mesylate: proposal of new computed tomography response criteria, J. Clin. Oncol. 25 (May (13)) (2007) 1753–1759 2006.07.3049.